



ELSEVIER

Available online at www.sciencedirect.com

SCIENCE @ DIRECT®

Journal of Sound and Vibration 283 (2005) 1031–1049

JOURNAL OF
SOUND AND
VIBRATION

www.elsevier.com/locate/jsvi

A novel time-domain auto-regressive model for structural damage diagnosis

Yong Lu*, Feng Gao

*School of Civil and Environmental Engineering, Nanyang Technological University,
Nanyang Avenue, Singapore 639798, Singapore*

Received 9 January 2004; received in revised form 26 April 2004; accepted 1 June 2004
Available online 11 November 2004

Abstract

In this paper, a novel time-series model is proposed for the diagnosis of structural damage. Two major issues need be addressed when considering time-domain data for damage detection; one is a damage sensitive feature and the other concerns the fact that the input excitation usually is not measurable. The present approach stems from the linear dynamic system theory and it is formulated in the form of a prediction model of auto-regressive with eXogenous input. With some simplifications, the model is expressed such that only response (acceleration) signals are involved, with response at one location chosen as the “input” of the model. The model coefficients correlate with the dynamic properties of the structure and they can be established from reference-state response signals. The residual error of the established model when applied on actually measured signals reflects the structural change, and the standard deviation of the residual error is found to be a damage sensitive feature. Numerical examples demonstrate that the method can be applied for a rapid detection of structural changes and it can also indicate the damage locations. Furthermore, the model can tolerate certain variation of the actual excitation. The model provides a basis for developing more robust damage sensitive features for real applications.

© 2004 Elsevier Ltd. All rights reserved.

*Corresponding author. Tel.: +65-790-5278; fax: +65-791-0676.
E-mail address: cylu@ntu.edu.sg (Y. Lu).

1. Introduction

As a general understanding, the presence of damage in a structure results in more or less significant change in its mechanical properties, which usually manifest themselves as a change in the measurable dynamic properties. For this reason, the commonly employed approaches to damage identification and diagnosis have stemmed from identification of the dynamic parameters, such as natural frequencies, mode shapes and damping coefficients. Methods for identification of the dynamic system parameters in turn can be broadly divided into two categories, namely, frequency domain methods and time-domain methods. The time-domain methods for system identification usually go through models of stochastic processes, for instance the auto-regressive moving average (ARMA) models.

As far as linear systems are concerned (in this sense the presence of damage is invariably assumed to have resulted in reduction of stiffness, and possibly inertia, characteristics of the structure whose behavior remains linear at the damaged state), the linear system theory states that the output response to a linear combination of inputs is the same linear combination of the output responses of the individual inputs. A general expression describing the relationship between input data $y(t)$, output data $u(t)$ and residual error $e(t)$ in the time-domain may be written as

$$A(q)y(t) = B(q)u(t) + C(q)e(t), \quad (1)$$

where A , B and C are polynomials in the delay operator q^{-1} :

$$A(q) = 1 + a_1q^{-1} + \cdots + a_{na}q^{-na},$$

$$B(q) = b_1 + b_2q^{-1} + \cdots + b_{nb}q^{-nb+1},$$

$$C(q) = 1 + c_1q^{-1} + \cdots + c_{nc}q^{-nc},$$

where the numbers na , nb and nc are the orders of the respective polynomials.

The auto-regressive (AR) model is obtained when $nb = nc = 0$. In this model, the previous values of response are used to calculate the present value. The ARMA model is obtained when $nb = 0$. Both AR and ARMA describe a stationary process of a system using response data only. The moving average (MA) part provides a way of representing the disturbance, and it effects as a filter for the residual error. The auto-regressive with eXogenous input (ARX) model corresponds to $nc = 0$. The auto-regressive and moving average with eXogenous input (ARMAX) model takes the complete form of Eq. (1).

The above linear models have been applied in the time-domain analysis in civil engineering [1–7]. In most cases, the AR models are applied as transfer functions of signals in lieu of FFT analysis. On fitting the models to measured response signals, the model coefficients can be estimated using statistical (least-squares) method, which are then used to identify the system dynamic parameters. The selection of the AR model order is also discussed in some previous studies [4–7]. Lee and Yun [8] investigated the ARMA model for the time-domain identification of the dynamic parameters of a linear multidegree-of-freedom structural system.

Apart from the application for dynamic system identification, the use of time-domain analysis in constructing time-series signature for direct damage diagnosis has also attracted attention in

recent years. As operation in the time domain does not require domain change, it provides a potentially effective alternative for rapid monitoring applications. Such kind of time-domain damage diagnosis methods usually start with the setting up of a “black box” model from the measurements of the undamaged structure. When the dynamic properties of the system are altered due to damage, larger prediction errors comparing to the actual measurement will occur; hence, by analyzing the prediction errors a suitable damage feature can be extracted for the diagnosis of the damage. Masri et al. [9] employed the neural network technique to set up their black box and used RMS error ratio as the damage feature. Sohn and Farrar [10] proposed a two-step AR-ARX (auto-regressive–auto-regressive with eXogenous) model to predict the time series and subsequently used the standard deviation (STD) ratio of the residual error to indicate the damage. These methods were demonstrated to be workable under the conditions examined, though a clear physical basis was not provided.

In exploiting the time-domain approach for rapid monitoring and diagnosis of structural damage, it is desired that some novel time-series signatures be constructed from the measured signals so that they are closely related to the system parameters, and at the same time, they can be made relatively independent from the external excitation to the structure. The model established on this basis is expected to be generally more sensitive to the degree and distribution of damage.

In the present study, a method is developed to construct a novel auto-regressive time-series signature for the diagnosis of structural damage. The model stems from the linear dynamics and is formulated in the form of the ARX model involving only the (acceleration) response data. The STD of the residual error when the reference model is applied on the measured response of an unknown state is used as a damage feature. Numerical examples are given to demonstrate the ability of the method for rapid diagnosis of damage in a structure.

2. Dynamic system formulation and derivation of the ARX model

For a structural system with n degrees of freedom (DOF), the dynamic equation of the system can be described by

$$\mathbf{M}_0 \ddot{\xi}(t) + \mathbf{C}_0 \dot{\xi}(t) + \mathbf{K}_0 \xi(t) = \mathbf{L}_0 \mathbf{u}(t), \quad (2)$$

where $\mathbf{u}(t)$ is the input vector of dimension m ; \mathbf{M}_0 , \mathbf{C}_0 , \mathbf{K}_0 are mass, damping, and stiffness matrices; \mathbf{L}_0 is the $n \times m$ input coefficient matrix. In a more general sense when only r DOFs are measured ($r < n$), the above matrices can be regarded as the projected mass, damping and stiffness matrices of order $r \times r$, and input coefficient matrix of order $r \times m$, respectively.

Eq. (2) can be rewritten as

$$\ddot{\xi}(t) + \mathbf{J} \dot{\xi}(t) + \mathbf{K} \xi(t) = \mathbf{L} \mathbf{u}(t), \quad (3)$$

where $\mathbf{J} = \mathbf{M}_0^{-1} \mathbf{C}_0$, $\mathbf{K} = \mathbf{M}_0^{-1} \mathbf{K}_0$, and $\mathbf{L} = \mathbf{M}_0^{-1} \mathbf{L}_0$.

Since the measurements are normally digitized as discrete time series, it is necessary to convert Eq. (3) into the corresponding discrete time equation. In order to set up the relationship between the input and the response components in discrete-time space, especially for multiinput and multioutput (MIMO) systems, we consider the state space equation. The continuous time state

space model can be written in a compact form as [11]

$$\begin{aligned} \dot{\mathbf{x}}(t) &= \mathbf{A}_c \mathbf{x}(t) + \mathbf{B}_c \mathbf{u}(t), \\ \mathbf{y}(t) &= \mathbf{C} \mathbf{x}(t) + \mathbf{D} \mathbf{u}(t) \end{aligned} \tag{4}$$

with the definition of

$$\mathbf{A}_c = \begin{bmatrix} 0 & \mathbf{I} \\ -\mathbf{K} & -\mathbf{J} \end{bmatrix}, \quad \mathbf{B}_c = \begin{bmatrix} 0 \\ \mathbf{L} \end{bmatrix}, \quad \mathbf{x}(t) = \begin{bmatrix} \xi(t) \\ \dot{\xi}(t) \end{bmatrix}.$$

Consider the observed responses $\mathbf{y}(t)$ to be accelerations, $\mathbf{y} = \ddot{\xi}(t)$, the coefficients \mathbf{C} and \mathbf{D} in Eq. (4) can be obtained as $\mathbf{C} = [-\mathbf{K} \quad -\mathbf{J}]$, $\mathbf{D} = \mathbf{L}$.

In discrete time state space, it is assumed that the input and response are constant over the time interval $k\Delta t \leq t < (k+1)\Delta t$, in which Δt is the sampling period. For discrete-time response and input signals $\mathbf{y}(k\Delta t)$ and $\mathbf{u}(k\Delta t)$, the discrete time equations corresponding to Eq. (4) can be obtained as [12]

$$\begin{aligned} \mathbf{x}(k+1) &= \mathbf{A} \mathbf{x}(k) + \mathbf{B} \mathbf{u}(k), \\ \mathbf{y}(k) &= \mathbf{C} \mathbf{x}(k) + \mathbf{D} \mathbf{u}(k), \end{aligned} \tag{5}$$

where $\mathbf{u}(k)$, $\mathbf{y}(k)$, and $\mathbf{x}(k)$ denote the sampled data at $t = k\Delta t$, and the coefficients can be expressed as [11]

$$\mathbf{A} = e^{\mathbf{A}_c \Delta t}, \tag{5a}$$

$$\mathbf{B} = \int_0^{\Delta t} e^{\mathbf{A}_c \tau} d\tau \mathbf{B}_c = (\mathbf{A} - \mathbf{I}) \mathbf{A}_c^{-1} \mathbf{B}_c. \tag{5b}$$

The discrete-time matrices \mathbf{A} and \mathbf{B} in Eq. (5) may be computed by the following series expansions:

$$\mathbf{A} = \mathbf{I} + \mathbf{A}_c \Delta t + \frac{1}{2!} (\mathbf{A}_c \Delta t)^2 + \frac{1}{3!} (\mathbf{A}_c \Delta t)^3 + \dots, \tag{6}$$

$$\mathbf{B} = \left[\mathbf{I} \Delta t + \frac{1}{2!} \mathbf{A}_c \Delta t^2 + \frac{1}{3!} \mathbf{A}_c^2 \Delta t^3 + \frac{1}{4!} \mathbf{A}_c^3 \Delta t^4 + \dots \right] \mathbf{B}_c. \tag{7}$$

Let the state equation be written in a slightly different form. Add and subtract the term $\mathbf{G} \mathbf{y}(k)$ with an arbitrary matrix \mathbf{G} to Eq. (5),

$$\mathbf{x}(k+1) = \mathbf{A} \mathbf{x}(k) + \mathbf{B} \mathbf{u}(k) + \mathbf{G} \mathbf{y}(k) - \mathbf{G} \mathbf{y}(k). \tag{8}$$

Substituting $\mathbf{y}(k)$ from Eq. (5) into the above,

$$\mathbf{x}(k+1) = (\mathbf{A} + \mathbf{G} \mathbf{C}) \mathbf{x}(k) + (\mathbf{B} + \mathbf{G} \mathbf{D}) \mathbf{u}(k) - \mathbf{G} \mathbf{y}(k). \tag{9}$$

Define

$$\bar{\mathbf{A}} = \mathbf{A} + \mathbf{G} \mathbf{C}, \tag{10a}$$

$$\bar{\mathbf{B}} = [\mathbf{B} + \mathbf{G} \mathbf{D} - \mathbf{G}] \tag{10b}$$

and

$$\mathbf{v}(k) = \begin{bmatrix} \mathbf{u}(k) \\ \mathbf{y}(k) \end{bmatrix}.$$

It follows that

$$\mathbf{x}(k + 1) = \bar{\mathbf{A}}\mathbf{x}(k) + \bar{\mathbf{B}}\mathbf{v}(k),$$

$$\mathbf{y}(k) = \mathbf{C}\mathbf{x}(k) + \mathbf{D}\mathbf{u}(k). \tag{10}$$

This is the state-space observer model of a dynamical system. Because matrix \mathbf{G} can be arbitrarily chosen, $\bar{\mathbf{A}}$ may be made as asymptotically stable as desired with a proper \mathbf{G} .

Solving for the output $\mathbf{y}(k)$ from Eq. (10) with zero initial condition in terms of the previous input $\mathbf{u}(i)$ and outputs $\mathbf{y}(i)$ yields

$$\hat{\mathbf{y}}(k) = \sum_{i=1}^k \mathbf{C}\bar{\mathbf{A}}^{i-1}\bar{\mathbf{B}}\mathbf{v}(k - i) + \mathbf{D}\mathbf{u}(k) \tag{11}$$

Define

$$\bar{\mathbf{Y}}_1 = \mathbf{C}\bar{\mathbf{B}},$$

$$\bar{\mathbf{Y}}_2 = \mathbf{C}\bar{\mathbf{A}}\bar{\mathbf{B}},$$

$$\bar{\mathbf{Y}}_k = \mathbf{C}\bar{\mathbf{A}}^{k-1}\bar{\mathbf{B}} \equiv [\bar{\mathbf{Y}}_k^{(1)} - \bar{\mathbf{Y}}_k^{(2)}]. \tag{12}$$

Substituting the above into (11) and rearranging yields

$$\hat{\mathbf{y}}(k) + \sum_{i=1}^k \bar{\mathbf{Y}}_i^{(2)}\mathbf{y}(k - i) = \sum_{i=1}^k \bar{\mathbf{Y}}_i^{(1)}\mathbf{u}(k - i) + \mathbf{D}\mathbf{u}(k). \tag{13}$$

Eq. (13) is commonly called the linear difference model for multiinput/multioutput, linear, time-invariant systems. It is also often referred to as the ARX model where AR refers to the AutoRegressive part (related to output data) and X refers to the eXogeneous part (related to input data). This form is commonly used in developing recursive system identification techniques [13].

Define the series equation of matrix \mathbf{X} as

$$\begin{aligned} \cos \mathbf{X} &= \frac{e^{i\mathbf{X}} + e^{-i\mathbf{X}}}{2} = \mathbf{I} - \frac{\mathbf{X}^2}{2!} + \frac{\mathbf{X}^4}{4!} + \dots, \\ \sin \mathbf{X} &= \frac{e^{i\mathbf{X}} - e^{-i\mathbf{X}}}{2i} = \mathbf{X} - \frac{\mathbf{X}^3}{3!} + \frac{\mathbf{X}^5}{5!} + \dots. \end{aligned} \tag{14}$$

They have the property [12]: $\cos^2 \mathbf{X} + \sin^2 \mathbf{X} = \mathbf{I}$.

We also have

$$\mathbf{K} = \mathbf{M}_0^{-1}\mathbf{K}_0 = \mathbf{\Phi}\mathbf{\Lambda}\mathbf{\Phi}^T,$$

where

$$\Lambda = \begin{bmatrix} \omega_1^2 & & & \\ & \omega_2^2 & & \\ & & \ddots & \\ & & & \omega_n^2 \end{bmatrix}$$

is the eigenvalue matrix ($\omega_i^2 = \lambda_i$), Φ is the eigenvector matrix. In dynamic problems ω_i and ϕ_i are, respectively, the natural (circular) frequencies and the mass-normalized mode shape matrix. For mass-normalized mode shape matrix, $\Phi^T = \Phi^{-1}$. It follows that $\mathbf{K} = \Phi\Lambda^{1/2}\Phi^T\Phi\Lambda^{1/2}\Phi^T = (\Phi\Lambda^{1/2}\Phi^T)^2$ and $\mathbf{K}^{1/2} = \Phi\Lambda^{1/2}\Phi^T$.

To simplify the formulation, it is assumed at this point that the system is undamped, hence \mathbf{A}_c in Eq. (4) can be expressed as

$$\mathbf{A}_c = \begin{bmatrix} \mathbf{0} & \mathbf{I} \\ -\mathbf{K} & \mathbf{0} \end{bmatrix}$$

and

$$\mathbf{A}_c^2 = \begin{bmatrix} -\mathbf{K} & \mathbf{0} \\ \mathbf{0} & -\mathbf{K} \end{bmatrix}, \quad \mathbf{A}_c^3 = \begin{bmatrix} \mathbf{0} & -\mathbf{K} \\ \mathbf{K}^2 & \mathbf{0} \end{bmatrix},$$

$$\mathbf{A}_c^4 = \begin{bmatrix} \mathbf{K}^2 & \mathbf{0} \\ \mathbf{0} & \mathbf{K}^2 \end{bmatrix}, \quad \mathbf{A}_c^5 = \begin{bmatrix} \mathbf{0} & \mathbf{K}^2 \\ -\mathbf{K}^3 & \mathbf{0} \end{bmatrix}, \dots$$

Then, by Eqs. (6) and (7) the matrices \mathbf{A} and \mathbf{B} can be calculated:

$$\begin{aligned} \mathbf{A} &= \begin{bmatrix} \mathbf{I} - \frac{1}{2!}\mathbf{K}\Delta t^2 + \frac{1}{4!}\mathbf{K}^2\Delta t^4 + \dots & \mathbf{I}\Delta t - \frac{1}{3!}\mathbf{K}\Delta t^3 + \frac{1}{5!}\mathbf{K}^2\Delta t^5 + \dots \\ -\mathbf{K}\Delta t + \frac{1}{3!}\mathbf{K}^2\Delta t^3 - \frac{1}{5!}\mathbf{K}^3\Delta t^5 + \dots & \mathbf{I} - \frac{1}{2!}\mathbf{K}\Delta t^2 + \frac{1}{4!}\mathbf{K}^2\Delta t^4 + \dots \end{bmatrix} \\ &= \begin{bmatrix} \cos(\mathbf{K}^{1/2}\Delta t) & \mathbf{K}^{-1/2} \sin(\mathbf{K}^{1/2}\Delta t) \\ -\mathbf{K}^{1/2} \sin(\mathbf{K}^{1/2}\Delta t) & \cos(\mathbf{K}^{1/2}\Delta t) \end{bmatrix}. \end{aligned} \tag{15}$$

$$\begin{aligned} \mathbf{B} &= \begin{bmatrix} \mathbf{I}\Delta t - \frac{1}{3!}\mathbf{K}\Delta t^3 + \frac{1}{5!}\mathbf{K}^2\Delta t^5 + \dots & \frac{1}{2!}\mathbf{I}\Delta t^2 - \frac{1}{4!}\mathbf{K}\Delta t^4 + \frac{1}{6!}\mathbf{K}^2\Delta t^6 + \dots \\ -\frac{1}{2!}\mathbf{K}\Delta t^2 + \frac{1}{4!}\mathbf{K}^2\Delta t^4 - \frac{1}{6!}\mathbf{K}^3\Delta t^6 + \dots & \mathbf{I}\Delta t - \frac{1}{3!}\mathbf{K}\Delta t^3 + \frac{1}{5!}\mathbf{K}^2\Delta t^5 + \dots \end{bmatrix} \mathbf{B}_c \\ &= \begin{bmatrix} \mathbf{K}^{-1/2} \sin(\mathbf{K}^{1/2}\Delta t) & \mathbf{K}^{-1}(\mathbf{I} - \cos(\mathbf{K}^{1/2}\Delta t)) \\ -\mathbf{I} + \cos(\mathbf{K}^{1/2}\Delta t) & \mathbf{K}^{-1/2} \sin(\mathbf{K}^{1/2}\Delta t) \end{bmatrix} \mathbf{B}_c \\ &= \begin{bmatrix} \mathbf{K}^{-1}(\mathbf{I} - \cos(\mathbf{K}^{1/2}\Delta t)) \\ \mathbf{K}^{-1/2} \sin(\mathbf{K}^{1/2}\Delta t) \end{bmatrix} \mathbf{L}. \end{aligned} \tag{16}$$

Let the matrix \mathbf{G} be chosen such that

$$\mathbf{G} = \begin{bmatrix} 2\mathbf{K}^{-1} \cos(\mathbf{K}^{1/2}\Delta t) \\ -\mathbf{K}^{-1/2}(\sin(\mathbf{K}^{1/2}\Delta t) - \sin^{-1}(\mathbf{K}^{1/2}\Delta t) \cos(\mathbf{K}^{1/2}\Delta t)) \end{bmatrix}. \quad (17)$$

Note that matrices \mathbf{K} , \mathbf{K}^{-1} , $\mathbf{K}^{-1/2}$, $\cos(\mathbf{K}^{1/2}\Delta t)$, $\sin(\mathbf{K}^{1/2}\Delta t)$ are all symmetrical, so the sequence of matrices in the multiplication operation may be changed, e.g., $\mathbf{K}^{-1} \cos(\mathbf{K}^{1/2}\Delta t) = \cos(\mathbf{K}^{1/2}\Delta t)\mathbf{K}^{-1}$.

The matrices in Eq. (10) become

$$\begin{aligned} \bar{\mathbf{A}} &= \mathbf{A} + \mathbf{GC} \\ &= \begin{bmatrix} -\cos(\mathbf{K}^{1/2}\Delta t) & \mathbf{K}^{-1/2} \sin(\mathbf{K}^{1/2}\Delta t) \\ -\mathbf{K}^{1/2} \cos^2(\mathbf{K}^{1/2}\Delta t) \sin^{-1}(\mathbf{K}^{1/2}\Delta t) & \cos(\mathbf{K}^{1/2}\Delta t) \end{bmatrix}. \end{aligned} \quad (18)$$

$$\begin{aligned} \bar{\mathbf{B}} &= [\mathbf{B} + \mathbf{GD} \quad -\mathbf{G}] \\ &= \begin{bmatrix} \mathbf{K}^{-1}(\mathbf{I} + \cos(\mathbf{K}^{1/2}\Delta t))\mathbf{L} & -2\mathbf{K}^{-1} \cos(\mathbf{K}^{1/2}\Delta t) \\ \mathbf{K}^{-1/2} \cos^2(\mathbf{K}^{1/2}\Delta t) \sin^{-1}(\mathbf{K}^{1/2}\Delta t)\mathbf{L} & \mathbf{K}^{-1/2}(\sin(\mathbf{K}^{1/2}\Delta t) - \cos^2(\mathbf{K}^{1/2}\Delta t)\sin^{-1}(\mathbf{K}^{1/2}\Delta t)) \end{bmatrix}. \end{aligned} \quad (19)$$

The matrix $\bar{\mathbf{A}}$ is asymptotically stable in the sense that it takes only a power of two for $\bar{\mathbf{A}}$ to decay completely, as $\bar{\mathbf{A}}^2 = \bar{\mathbf{A}}^3 = \dots = \bar{\mathbf{A}}^n = \mathbf{0}$.

Substituting the matrices $\bar{\mathbf{A}}$, $\bar{\mathbf{B}}$ into Eq. (12), and noting $\mathbf{J} = \mathbf{0}$ (and hence $\mathbf{C} = [-\mathbf{K} \quad \mathbf{0}]$), we have

$$\begin{aligned} \bar{\mathbf{Y}}_1 &= \mathbf{C}\bar{\mathbf{B}} = [-(\mathbf{I} + \cos(\mathbf{K}^{1/2}\Delta t))\mathbf{L} \quad 2 \cos(\mathbf{K}^{1/2}\Delta t)], \\ \bar{\mathbf{Y}}_2 &= \mathbf{C}\bar{\mathbf{A}}\bar{\mathbf{B}} = [\cos(\mathbf{K}^{1/2}\Delta t)\mathbf{L} \quad -\mathbf{I}], \\ \bar{\mathbf{Y}}_3 &= \mathbf{C}\bar{\mathbf{A}}\bar{\mathbf{A}}\bar{\mathbf{B}} = [\mathbf{0} \quad \mathbf{0}], \\ \bar{\mathbf{Y}}_i &= \mathbf{C}\bar{\mathbf{A}}^{i-1}\bar{\mathbf{B}} = [\mathbf{0} \quad \mathbf{0}] \quad \text{for } i > 3. \end{aligned} \quad (20)$$

Then the ARX model in Eq. (13) can be written as

$$\begin{aligned} \hat{\mathbf{y}}(k) - 2 \cos(\mathbf{K}^{1/2}\Delta t)\mathbf{y}(k-1) + \mathbf{y}(k-2) &= -(\mathbf{I} + \cos(\mathbf{K}^{1/2}\Delta t))\mathbf{L}\mathbf{u}(k-1) \\ &\quad + \cos(\mathbf{K}^{1/2}\Delta t)\mathbf{L}\mathbf{u}(k-2) + \mathbf{L}\mathbf{u}(k). \end{aligned} \quad (21)$$

Since $\mathbf{K}^{1/2} = \mathbf{\Phi}\mathbf{\Lambda}^{1/2}\mathbf{\Phi}^T$, $\cos(\mathbf{K}^{1/2}\Delta t)$ can be rewritten as

$$\begin{aligned} \cos(\mathbf{K}^{1/2}\Delta t) &= \mathbf{I} - \frac{1}{2!}(\mathbf{K}^{1/2}\Delta t)^2 + \frac{1}{4!}(\mathbf{K}^{1/2}\Delta t)^4 + \dots \\ &= \mathbf{I} - \mathbf{\Phi}\left(\frac{1}{2!}(\mathbf{\Lambda}^{1/2}\Delta t)^2\right)\mathbf{\Phi}^T + \mathbf{\Phi}\left(\frac{1}{4!}(\mathbf{\Lambda}^{1/2}\Delta t)^4\right)\mathbf{\Phi}^T + \dots \\ &= \mathbf{\Phi}\left(\mathbf{I} - \frac{1}{2!}(\mathbf{\Lambda}^{1/2}\Delta t)^2 + \frac{1}{4!}(\mathbf{\Lambda}^{1/2}\Delta t)^4 + \dots\right)\mathbf{\Phi}^T \\ &= \mathbf{\Phi} \cos(\mathbf{\Lambda}^{1/2}\Delta t)\mathbf{\Phi}^T. \end{aligned} \quad (22)$$

Here

$$\cos \Lambda^{1/2} \Delta t = \begin{bmatrix} \cos \omega_1 \Delta t & & 0 \\ & \ddots & \\ 0 & & \cos \omega_n \Delta t \end{bmatrix}. \tag{22a}$$

Subsequently, Eq. (21) can be expressed as ARX model:

$$\mathbf{y}(k) = \mathbf{P}_1 \mathbf{y}(k-1) + \mathbf{P}_2 \mathbf{y}(k-2) + \mathbf{D} \mathbf{u}(k) + \mathbf{E}_1 \mathbf{u}(k-1) + \mathbf{E}_2 \mathbf{u}(k-2), \tag{23}$$

where

$$\mathbf{P}_1 = 2\mathbf{\Phi} \cos(\Lambda^{1/2} \Delta t) \mathbf{\Phi}^T, \tag{23a}$$

$$\mathbf{P}_2 = -\mathbf{I}, \tag{23b}$$

$$\mathbf{D} = \mathbf{L}, \tag{23c}$$

$$\mathbf{E}_1 = -\mathbf{\Phi} [\mathbf{I} + \cos(\Lambda^{1/2} \Delta t)] \mathbf{\Phi}^T \mathbf{L}, \tag{23d}$$

$$\mathbf{E}_2 = \mathbf{\Phi} \cos(\Lambda^{1/2} \Delta t) \mathbf{\Phi}^T \mathbf{L}. \tag{23e}$$

It should be noted that the above explicit expression between the ARX model coefficients and the system dynamic properties have been derived for undamped systems. In such cases, once the coefficient matrices $[\mathbf{P}_1, \mathbf{P}_2, \mathbf{D}, \mathbf{E}_1, \mathbf{E}_2]$ of the ARX model are estimated from a given set of response and input time series data following a standard least-squares procedure, the dynamic system parameters $[\mathbf{J}, \mathbf{K}, \mathbf{L}]$ may be recovered through a numerical procedure. For damped systems, Lee and Yun [8] also obtained a similar expression of the ARX model as Eq. (23). In that case, however, the model coefficient matrices are no longer related to the system dynamic properties in an explicit manner as shown in Eqs. (23a–e). Nevertheless, the ARX model expressed in Eq. (23) can still be used for constructing the time-series damage feature for diagnosis purpose, as will be demonstrated later.

It is possible to eliminate the external excitation input from the ARX model for cases whereby the excitation comes from one single source, either as force excitation with a single forcing function or base excitation. In such cases, $\mathbf{u}(k)$ reduces to a single time series, and \mathbf{L} becomes a column with n rows. Subsequently, Eq. (23) can be written as

$$\mathbf{y}(k) = \mathbf{P}_1 \mathbf{y}(k-1) + \mathbf{P}_2 \mathbf{y}(k-2) + \mathbf{L} u(k) + \mathbf{E}_1 u(k-1) + \mathbf{E}_2 u(k-2). \tag{24}$$

Suppose the excitation acts on j th dof (or simply take the j th dof as a reference point in case of base excitation), then the collocated response at the same dof, j , can be written as

$$y_j(k) = l_j u(k) + \sum_{i=1}^n p_{1,ji} y_i(k-1) + \sum_{i=1}^n p_{2,ji} y_i(k-2) + e_{1,j} u(k-1) + e_{2,j} u(k-2). \tag{25}$$

As l_j is not zero, $u(k)$ can be expressed as

$$u(k) = \frac{1}{l_j} \left[y_j(k) - \sum_{i=1}^n p_{1,ji} y_i(k-1) - \sum_{i=1}^n p_{2,ji} y_i(k-2) - e_{1,j} u(k-1) - e_{2,j} u(k-2) \right]. \tag{26}$$

Define $\bar{\mathbf{y}}$ as vector

$$\bar{\mathbf{y}} = \{y_1 \quad \cdots \quad y_{j-1} \quad y_{j+1} \quad \cdots \quad y_i\}^T,$$

$$\begin{aligned} \bar{\mathbf{y}}(k) &= \bar{\mathbf{P}}_1 \mathbf{y}(k-1) + \bar{\mathbf{P}}_2 \mathbf{y}(k-2) + \bar{\mathbf{L}} u(k) + \bar{\mathbf{E}}_1 u(k-1) + \bar{\mathbf{E}}_2 u(k-2) \\ &= \bar{\mathbf{P}}_1 \mathbf{y}(k-1) + \bar{\mathbf{P}}_2 \mathbf{y}(k-2) + \bar{\mathbf{E}}_1 u(k-1) + \bar{\mathbf{E}}_2 u(k-2) \\ &\quad + \frac{\bar{\mathbf{L}}}{l_j} \left(y_j(k) - \sum_{i=1}^n p_{1,ji} y_i(k-1) - \sum_{i=1}^n p_{2,ji} y_i(k-2) - e_{1,j} u(k-1) - e_{2,j} u(k-2) \right) \\ &= \bar{\mathbf{P}}_1 \mathbf{y}(k-1) + \bar{\mathbf{P}}_2 \mathbf{y}(k-2) + \frac{\bar{\mathbf{L}}}{l_j} y_j(k) - \frac{\bar{\mathbf{L}}}{l_j} \sum_{i=1}^n p_{1,ji} y_i(k-1) - \frac{\bar{\mathbf{L}}}{l_j} \sum_{i=1}^n p_{2,ji} y_i(k-2) \\ &\quad + \left(\bar{\mathbf{E}}_1 - \frac{\bar{\mathbf{L}}}{l_j} e_{1,j} \right) u(k-1) + \left(\bar{\mathbf{E}}_2 - \frac{\bar{\mathbf{L}}}{l_j} e_{2,j} \right) u(k-2), \end{aligned} \tag{27}$$

where matrices $\bar{\mathbf{P}}_1, \bar{\mathbf{P}}_2$ refer to the matrices \mathbf{P}_1 and \mathbf{P}_2 without j th row; and vectors $\bar{\mathbf{L}}, \bar{\mathbf{E}}_1$ and $\bar{\mathbf{E}}_2$ are vectors \mathbf{L}, \mathbf{E}_1 and \mathbf{E}_2 without j th element.

Under the condition that $\omega_n \Delta t$ is small enough (for relatively stiff systems, this would require a sufficiently small Δt), the matrix $\cos(\Lambda^{1/2} \Delta t)$ as expressed in Eq. (22a) will approach an identity matrix. According to Eqs. (23d)–(23e), it follows that $\mathbf{E}_1 \approx -2\mathbf{L}, \mathbf{E}_2 \approx \mathbf{L}, \bar{\mathbf{E}}_1 \approx -2\bar{\mathbf{L}}, \bar{\mathbf{E}}_2 \approx \bar{\mathbf{L}}$ and $e_{1,j} \approx -2l_{1,j}, e_{2,j} \approx l_{2,j}$. Then in Eq. (27) the coefficients of $u(k-1)$ and $u(k-2)$ approaches zero, and subsequently the equation reduces to include only the time series $\mathbf{y}(k-1), \mathbf{y}(k-2), y_j(k), y_j(k-1)$ and $y_j(k-2)$, without the excitation terms. Now the model can be written in ARX form without the excitation term, as

$$\bar{\mathbf{y}}(k) = \mathbf{A}_1 \bar{\mathbf{y}}(k-1) + \mathbf{A}_2 \bar{\mathbf{y}}(k-2) + \mathbf{B}_0 y_j(k) + \mathbf{B}_1 y_j(k-1) + \mathbf{B}_2 y_j(k-2) + \mathbf{e}(k), \tag{28}$$

where $\mathbf{e}(k)$ denotes the residual error of the model, and

$$\mathbf{A}_1 = \begin{bmatrix} p1_{1,1} & \cdots & p1_{1,j-1} & p1_{1,j+1} & \cdots & p1_{1,n} \\ \vdots & \ddots & \vdots & \vdots & \ddots & \vdots \\ p1_{j-1,1} & \cdots & p1_{j-1,j-1} & p1_{j-1,j+1} & \cdots & p1_{j-1,n} \\ p1_{j+1,1} & \cdots & p1_{j+1,j-1} & p1_{j+1,j+1} & \cdots & p1_{j+1,n} \\ \vdots & \ddots & \vdots & \vdots & \ddots & \vdots \\ p1_{n,1} & \cdots & p1_{n,j-1} & p1_{n,j+1} & \cdots & p1_{n,n} \end{bmatrix} - \frac{\bar{\mathbf{L}}}{l_j} [p1_{j,1} \quad \cdots \quad p1_{j,j-1} \quad p1_{j,j+1} \quad \cdots \quad p1_{j,n}],$$

$$\mathbf{A}_2 = \begin{bmatrix} p2_{1,1} & \cdots & p2_{1,j-1} & p2_{1,j+1} & \cdots & p2_{1,n} \\ \vdots & \ddots & \vdots & \vdots & \ddots & \vdots \\ p2_{j-1,1} & \cdots & p2_{j-1,j-1} & p2_{j-1,j+1} & \cdots & p2_{j-1,n} \\ p2_{j+1,1} & \cdots & p2_{j+1,j-1} & p2_{j+1,j+1} & \cdots & p2_{j+1,n} \\ \vdots & \ddots & \vdots & \vdots & \ddots & \vdots \\ p2_{n,1} & \cdots & p2_{n,j-1} & p2_{n,j+1} & \cdots & p2_{n,n} \end{bmatrix} \\
 + \frac{\bar{\mathbf{L}}}{l_j} [p2_{j,1} \quad \cdots \quad p2_{j,j-1} \quad p2_{j,j+1} \quad \cdots \quad p2_{j,n}], \\
 \mathbf{B}_0 = \frac{\bar{\mathbf{L}}}{l_j}, \quad \mathbf{B}_1 = -\frac{p1_{j,j}}{l_j} \bar{\mathbf{L}} + [p1_{1,j} \quad \cdots \quad p1_{j-1,j} \quad p1_{j+1,j} \quad \cdots \quad p1_{n,j}]^T, \\
 \mathbf{B}_2 = -\frac{p2_{j,j}}{l_j} \bar{\mathbf{L}} + [p2_{1,j} \quad \cdots \quad p2_{j-1,j} \quad p2_{j+1,j} \quad \cdots \quad p2_{n,j}]^T.$$

Measurements taken from the undamaged structure can be used as reference signals to estimate the coefficient matrices of the ARX model through a standard procedure of the least-squares approach [14]. As the coefficients \mathbf{A}_1 , \mathbf{A}_2 , \mathbf{B}_0 , \mathbf{B}_1 and \mathbf{B}_2 of the ARX model are functions of the dynamic parameters; they may be employed for the system identification purpose. The present study, however, focuses on the capability of the above-derived ARX model as a time series analysis tool for the damage diagnosis of structural systems. Owing to the inherent relationship with the underlying dynamic system, it is expected that this model is sensitive to the changes of the physical parameters (stiffness in particular). Furthermore, as there is no excitation term involved, the model should be more robust in tolerating certain variation in the actual excitation so that the prediction errors are primarily attributable to the change of the structural properties.

In the subsequent numerical investigation, it will be shown that the STD of the residual errors in the predicted signals for an actually measured state, $\sigma(e_m)$, as compared to the STD of the residual error for the reference (undamaged) state, $\sigma(e_0)$, is a suitable feature for the diagnosis of damage. For MDOF systems, larger residual errors occur at the measurement points closer to the damage, and this enables the detection of the damage location. It will also be shown that the present model has much improved sensitivity to the structural stiffness change as compared to a previous two-step time-series model.

3. Application of the new ARX model and numerical examples

In order to investigate the effectiveness of the proposed model, a numerical simulation study is conducted. Two structural models are considered, one is a 2-dof mass–spring system and another is an 8-dof system. Random excitations are generated from either Gaussian white noise or random

noise. Three random series are used, namely, (1) Wtn-1 (White noise), with a standard deviation of 1.1287, (b) Randn-1 (random noise), with a standard deviation of 1.0040, and (c) Randn-2, which has two-times larger magnitude than the Randn-1. The sampling time step Δt is 0.01 s and the number of data points is chosen to be 4000 for each sample piece. The same time step and duration are used in recording the response signals from the simulation. The unit of input time series is kN for force excitation and m/s^2 for base excitation.

3.1. Two-dof system

The 2-dof mass spring model is depicted in Fig. 1, without or with damping (assuming 5% damping ratio). Each point mass is 419.4 kg and the initial spring stiffness k_1 and k_2 are both equal to 56.7 kNm^{-1} . The natural periods of the system without damping are calculated to be $T_1 = 0.874 \text{ s}$ and $T_2 = 0.334 \text{ s}$. The excitation on the structure is imposed at the base by random acceleration described above.

The acceleration responses at m_1 and m_2 , denoted as y_1 and y_2 , are recorded from the numerical simulations. According to Eq. (28), the ARX model of this system can be written as

$$y_2(k) = A_1y_2(k - 1) + A_2y_2(k - 2) + B_0y_1(k) + B_1y_1(k - 1) + B_2y_1(k - 2) + e(k).$$

Using the responses at m_1 and m_2 , a least-squares approach is applied to determine the model coefficients. The procedure is performed using Matlab system identification toolbox. Taking the excitation case Wtn1 for example, the ARX model coefficients for the original (reference) system are found to be: $A_1 = 1.973$, $A_2 = 1.000$, $B_0 = 1.002$, $B_1 = -1.964$, and $B_2 = 1.002$. The STD of the residual error, $\sigma(e_0)$, is found to be $9.6301e-06$. The coefficients for the system under the other two base excitations are almost the same as the above. Each of the above three ARX models are then used on the system response under the other two excitations. Table 1 summarizes the STDs

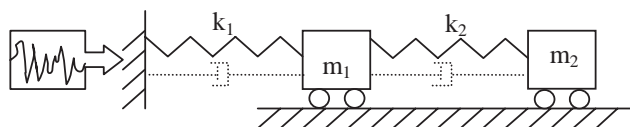


Fig. 1. Two-dof dynamic system without/with damping: (a) reference state; (b) damaged state (scenario (b)—20% stiffness reduction).

Table 1
STD of residual error for the undamaged state of the 2-dof system under different input excitations

Reference model	Undamped system			5%-Damped system		
	Wtn-1	Randn-1	Randn-2	Wtn-1	Randn-1	Randn-2
Wtn-1	9.6301e-006	9.7156e-006	1.0098e-005	9.8948e-006	9.7179e-006	9.6089e-006
Randn-1	9.6347e-006	9.7120e-006	1.0090e-005	9.0647e-006	9.9095e-006	9.6347e-006
Randn-2	9.6286e-006	9.7030e-006	1.0037e-005	9.6054e-006	9.8959e-006	9.7136e-006

of the residual errors for all the 9 combinations. Similarly, for the 5%-damped system, the ARX models are constructed based on the respective response data, and the residual errors are also shown in Table 1.

As can be seen from Table 1, all the residual errors are very small, and they are very close to each other regardless whether the excitation is the same as that used for establishing the reference model. In other words, each ARX model is able to predict the response signals under different excitations with practically the same accuracy. This behavior is significant in the sense that once the ARX model is established using signals from a particular random excitation, it can be applied for diagnosis purpose without requiring exactly the same type of excitation. Besides, for the damped system, the ARX model can be established to a comparable degree of satisfaction as that for the undamped system.

Now three damage scenarios are introduced: (a) the stiffness of k_1 is reduced by 10%; (b) the stiffness of k_1 is reduced by 20%; and (c) a bumper is inserted between m_1 and m_2 to cause nonlinear response. The bumper effect is simulated by a nonlinear element of a gap nature with an opening of 0.01 m and a compressive stiffness of 500 kN m^{-1} upon the closing of the gap. For each damage scenario, the system is subjected, respectively, to the aforementioned base excitations and the response at m_1 and m_2 are recorded. The response signals are then fed to the reference ARX models to predict the response at m_2 and the corresponding residual errors are obtained. Subsequently, the STD of the residual errors, $\sigma(e_m)$, are calculated and compared with reference STD error, $\sigma(e_0)$. Table 2 shows the STD ratios, $\sigma(e_m)/\sigma(e_0)$, for the various damage scenarios. Included in the table is also a damage scenario for the damped system for illustrative purpose.

From Table 2, it can be clearly observed that the residual error when using the reference ARX model on the damaged structure is 2–5 orders of magnitude higher than the reference residual error. This indicates that the model is sensitive to the presence of damage in the dynamic system. In general, higher residual errors occur for larger degree of damage, while the presence of nonlinearity in the measured signals results in a further increased residual error. For the same state of the structure, the residual errors from different excitations are not exactly the same,

Table 2
Residual error STD ratios, $\sigma(e_m)/\sigma(e_0)$, for various damage scenarios of the 2-dof system

Reference model	Undamped system		5%-Damped system	
	Wtn-1	Randn-1	Wtn-1	Randn-1
Scenario (a): 10% stiffness reduction				
Wtn-1	6.023e+2	7.269e+2	3.177e+2	3.226e+2
Randn-1	6.020e+2	7.265e+2	3.238e+2	3.289e+2
Scenario (b): 20% stiffness reduction				
Wtn-1	1.121e+3	1.879e+3		
Randn-1	1.121e+3	1.878e+3		
Scenario (c): bumper				
Wight-1	2.637e+5	3.852e+5		
Random-1	2.623e+5	3.832e+5		

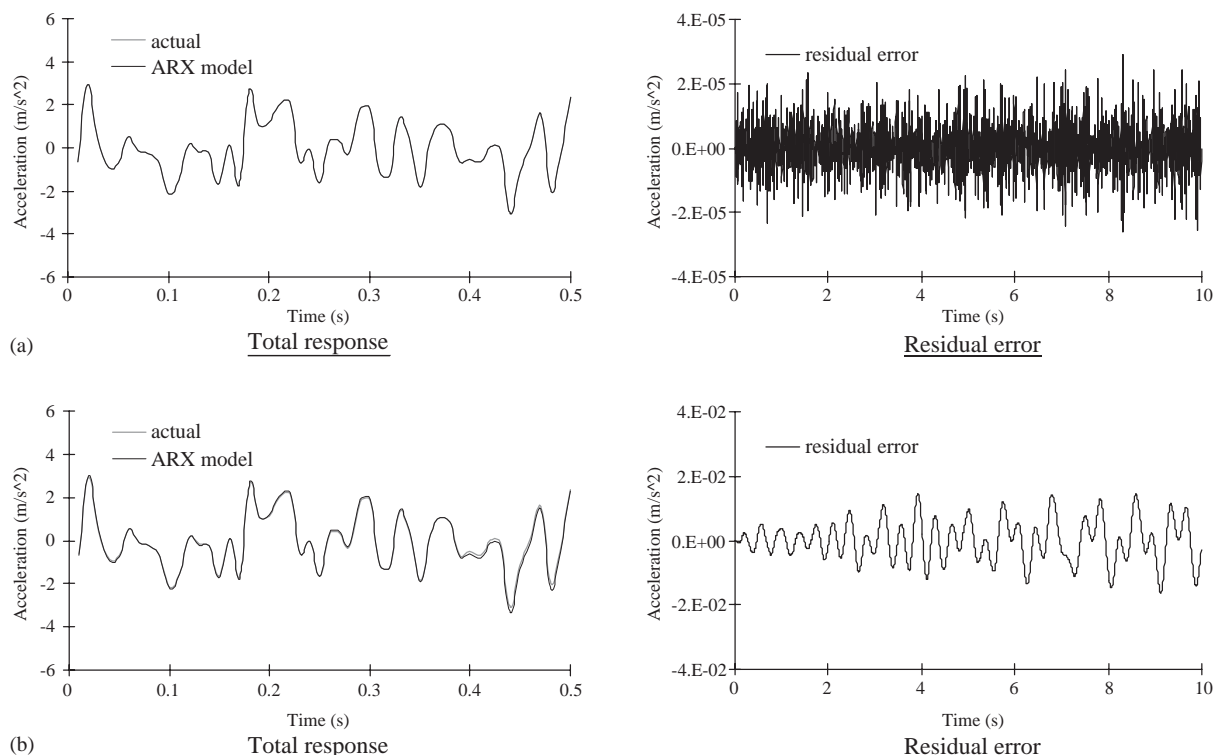


Fig. 2. Typical time histories of simulated and predicted acceleration responses and residual errors. (a) Reference state; (b) damaged state (Scenario (b): 20% stiffness reduction).

but maintain a good consistency. For a damped system with damage represented by a stiffness change (e.g., the 10% stiffness reduction case), the presence of damage can also be detected by the considerable increase of the prediction residual error using the respective reference model, although the magnitude of the residual error STD ratio is somewhat lower as compared to the undamped situation.

Fig. 2 shows a typical comparison of the ARX predicted and the actual response time histories for the reference state and a damaged state. To highlight the residual errors, the error histories are also plotted in the figure. As can be seen, the reference residual error is very small and it shows an apparent random characteristic. On the contrary, the residual error when the model is applied on the damaged state is considerably larger; and moreover, its waveform clearly contains the system response as opposed to the random error at the reference state. This feature tends to imply that it may be possible to deduce more detailed damage information from the system response content in the residual error for the damaged state, in addition to what can be understood from the increased magnitude of the error. Further study is to be conducted to analyze the feature of the residual error for a damaged state in a more comprehensive manner.

The subsequent example will demonstrate the ability of the model in detecting the location, as well as the presence, of damage in an mdof system.

3.2. Eight-dof system

3.2.1. General description

An 8-dof mass spring system is set up, as shown in Fig. 3, to investigate the applicability of the proposed model in mdof systems and its ability in locating the damage. The system has uniform mass of 419.4 kg at each node and a uniform spring stiffness of 56.7 kN m⁻¹ throughout. The first three natural periods of the system are calculated to be $T_1 = 2.931$ s, $T_2 = 0.9882$ s and $T_3 = 0.6067$ s. Two excitation schemes are considered, one is by acceleration from the base, and another is by a random force acting at m_1 which is closest to the base. For each excitation scheme, both Wtn1 and Randn1 are used as the excitation input. The force excitation scheme is included for the consideration that a controlled random force excitation at a dof would be easier to perform in practice; especially, for civil engineering structures. Since the vibration input to the structure is not required in the current method, it is expected that both excitation schemes would lead to similar diagnosis results. It should be noted that, as the input coefficient matrix L_0 in Eq. (2) are different under different excitation schemes, the respective model coefficients will relate to the system's dynamic properties in different ways; this to a certain extent could affect the model sensitivity.

After all the acceleration response signals are simulated by means of a dynamic analysis, the ARX models of Eq. (28) are established. When the response at m_1 is used as “input”, and the response at other locations are regarded as “output”, the ARX model is expressed as

$$\bar{y}(k) = \mathbf{A}_1 \bar{y}(k-1) + \mathbf{A}_2 \bar{y}(k-2) + \mathbf{B}_0 y_1(k) + \mathbf{B}_1 y_1(k-1) + \mathbf{B}_2 y_1(k-2) + \mathbf{e}(k),$$

where $\bar{y}(k) = \{y_2(k), \dots, y_8(k)\}^T$, $y_1 \sim y_8$ are acceleration responses at joints m_1 to m_8 , respectively, and $\mathbf{e}(k)$ is a 7-row residual error vector.

Table 3 shows the STD of the reference residual errors (undamaged state) at the 7 mass points for the two excitation schemes. It is noted that with the second excitation scheme (force excitation at m_1) the STD at m_2 is larger than those at other locations. This reflects that the response at this point is somehow masked by the excitation input that takes place at the adjacent point m_1 .

3.2.2. Damage at locations away from the “input” response point

When one spring stiffness has been altered, the largest increase in the residual error (in terms of STD) is expected to occur at the nearest measurement points. Here two damage scenarios are simulated, respectively, namely: (1) case-a: the stiffness of spring k_7 between m_6 and m_7 is reduced by 20%, and (2) case-b: the stiffness of spring k_3 between m_2 and m_3 is reduced by 20%. Four sets of responses are simulated for each damage scenario; two under base excitations of Wtn1 and Randn1, and two under the exciting forces of Wtn1 and Randn1 at m_1 . Figs. 4 and 5 show the

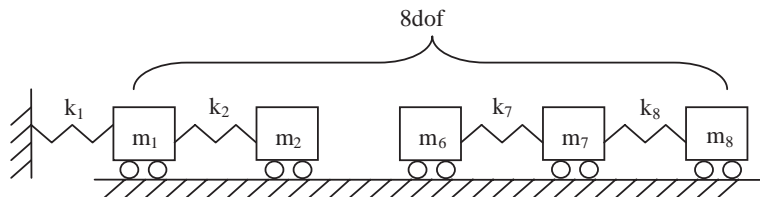


Fig. 3. The eight-dof system.

Table 3
STD of residual errors for the undamaged 8-dof system by two excitation methods

Reference model	y_2	y_3	y_4	y_5	y_6	y_7	y_8
<i>By base excitation</i>							
Wtn-1 $\sigma(e_0)$	5.1259e-5	5.1311e-5	5.1328e-5	5.1333e-5	5.1322e-5	5.1318e-5	5.1292e-5
Randn-1	5.5282e-5	5.5391e-5	5.5366e-5	5.5376e-5	5.5339e-5	5.5384e-5	5.5375e-5
<i>By random force acting on m_1</i>							
Wtn-1 $\sigma(e_0)$	1.2018e-4	6.9199e-6	6.9898e-6	6.7692e-6	7.0903e-6	7.1103e-6	6.9457e-6
Randn-1	1.3008e-4	7.1687e-6	6.943e-6	7.1435e-6	7.0635e-6	6.7957e-6	6.9499e-6

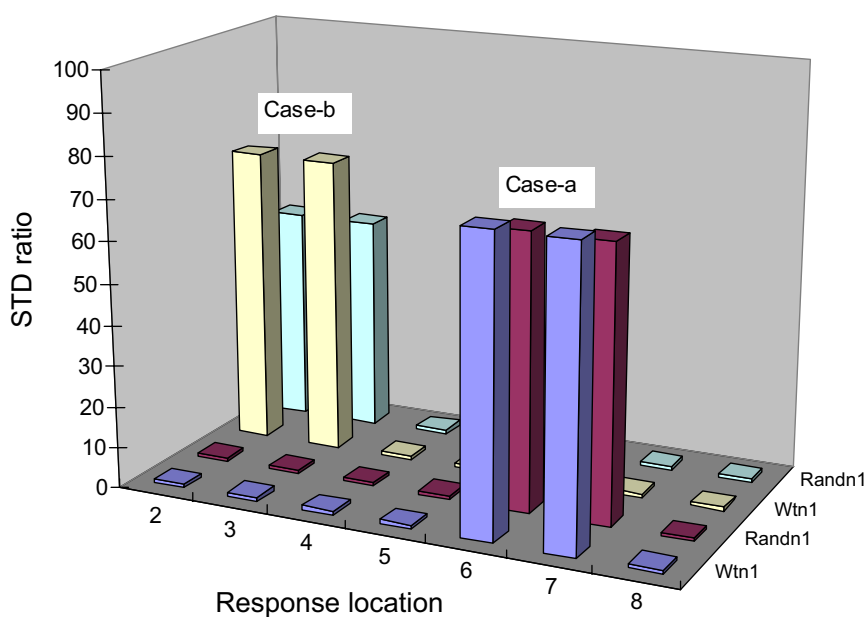


Fig. 4. STD ratio ($\sigma(e_m)/\sigma(e_0)$) for two damage scenarios by base excitation.

STD ratios of the residual errors between the damaged and the original reference states under base excitation and force excitation, respectively.

From Figs. 4 and 5 the locations of damage can be clearly identified since the STD ratio of the residual errors increase abruptly at the points near the damage. Both excitation methods can provide good diagnosis, except that in the case of forced excitation imposed at m_1 (see Fig. 5), the response at the adjacent point m_2 is not so sensitive to damage at the nearby k_3 , due to the “masking” effect mentioned earlier. Overall, the proposed ARX model is able to detect the locations of the damage in the mdof system.

To highlight the improvement of the present method in detecting this kind of damage, a comparison is made between the performance of the present model as shown above and the model proposed by Sohn and Farrar [2]. Their model is essentially a two-step AR-ARX model. The

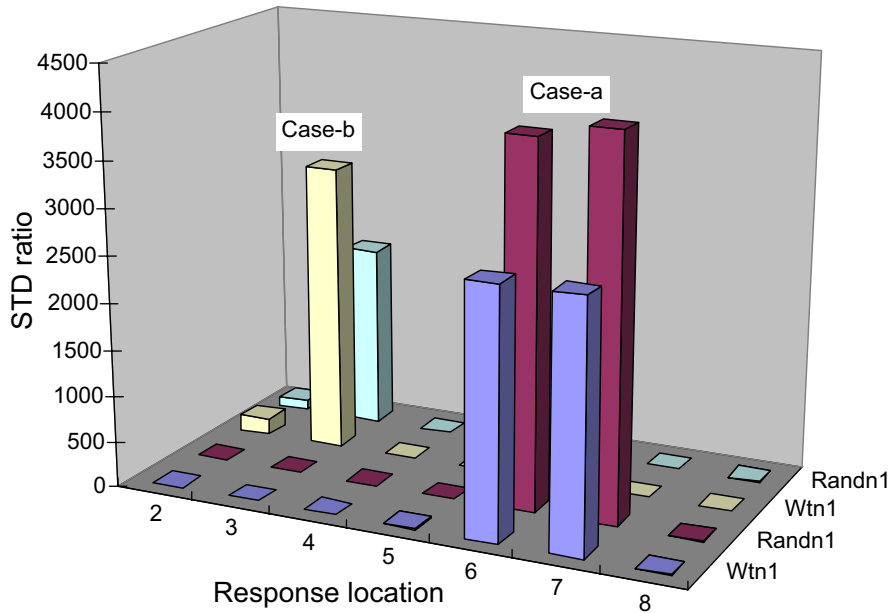


Fig. 5. STD ratio ($\sigma(e_m)/\sigma(e_0)$) for two damage scenarios by force excitation at m_1 .

Table 4
STD ratios from the two-step AR-ARX model

Damage scenario	y_1	y_2	y_3	y_4	y_5	y_6	y_7	y_8
Case-a	0.993	1.003	0.998	1.001	1.002	1.010	0.998	0.999
Case-b	1.005	1.018	1.010	1.007	1.002	1.001	1.009	1.005

procedure analyzes the acceleration response of each point independently. In the first step, the signal is predicted by an AR model; then, the signal is predicted by an ARX model using the residual error of the AR model in the first step as the eXogenous input. The STD of errors between the predicted signals in the second step and the measured signals are used as the damage feature to detect and locate the damage. The method has been shown [2] to work out quite successfully for cases where nonlinearity (such as a bumper) is involved in the measured response signals.

Table 4 shows the STD ratios from the above two-step model when it is applied on the 8-dof system under consideration, for two stiffness degradation scenarios (case-a and case-b). Note that only the results from the base excitation scheme are presented. As can be seen, the damage features (STD ratios) are almost identical at all measurement points and they are close to unity, which means no damage is detected while stiffness degradation actually took place, respectively, at two individual springs. In comparison, the results from the present ARX model, as described

earlier, clearly capture the presence and the location of the damage regardless whether it is a stiffness degradation or a nonlinear effect.

3.3.3. Damage at locations near the “input” response point

In this section, it will be shown that when the damage location is close to the point from which the response signal is taken as “input” to the ARX model, the diagnosis could be complicated. For this purpose, two more damage scenarios are simulated, one (case-c) is a degradation of stiffness by 20% at spring k_2 between m_2 and m_3 ; the other (case-d) is a degradation of stiffness by 20% at spring k_1 between m_1 and the base support. The response at m_1 is again used as the “input” in the ARX model.

Table 5 shows the STD ratios of the residual errors for the damaged structure when the excitation is imposed from the base. For damage at k_2 (case-c), the STD ratios at all points are very large. Although the damage at k_2 still appears to be detectable as the residual error at m_2 (y_2) is higher than the remaining errors, the high STD ratios at all locations tend to indicate an abnormal behavior of the model. This is further evidenced in the case of damage at k_1 (case-d), for which all points show large residual errors and no clear pattern is observed.

Table 6 shows the STD ratios when the system is subjected to a force excitation at m_2 . It can be seen that when damage occurs at k_2 , it is detectable because only the STD ratio at m_2 is significantly large. When damage is at k_1 , however, no feature appears to reflect the occurrence and location of the damage.

Apparently, the abnormal behavior of the model for the above cases is associated with the fact that the location of the damage is close to the response point that is used as “input” of the ARX model. As such, a natural way to get rid of the problem would be carrying out two separate runs of the procedure using two different “input” response locations. A correct detection of any arbitrary damage location should be achieved by inspecting the results from both runs.

As an example, when the response at m_8 is used as the “input”, the model becomes

$$\bar{y}(k) = \mathbf{A}_1\bar{y}(k - 1) + \mathbf{A}_2\bar{y}(k - 2) + \mathbf{B}_0y_8(k) + \mathbf{B}_1y_8(k - 1) + \mathbf{B}_2y_8(k - 2) + \mathbf{e}(k),$$

Table 5
STD ratios of the damaged 8-dof system by base excitation

Damage scenario	y_2	y_3	y_4	y_5	y_6	y_7	y_8
Case-c	2.18e+02	1.09e+02	1.09e+02	1.09e+02	1.09e+02	1.09e+02	1.09e+02
Case-d	6.83e+01	7.02e+01	7.01e+01	7.01e+01	7.01e+01	7.02e+01	7.02e+01

Table 6
STD ratios of the damaged 8-dof system by force excitation at m_1

Damage scenario	y_2	y_3	y_4	y_5	y_6	y_7	y_8
Case-c	2.48e+02	5.80e+00	1.31e+00	1.35e+00	1.28e+00	1.28e+00	1.10e+00
Case-d	1.01e+00	1.07e+00	1.06e+00	1.11e+00	1.06e+00	1.06e+00	1.03e+00

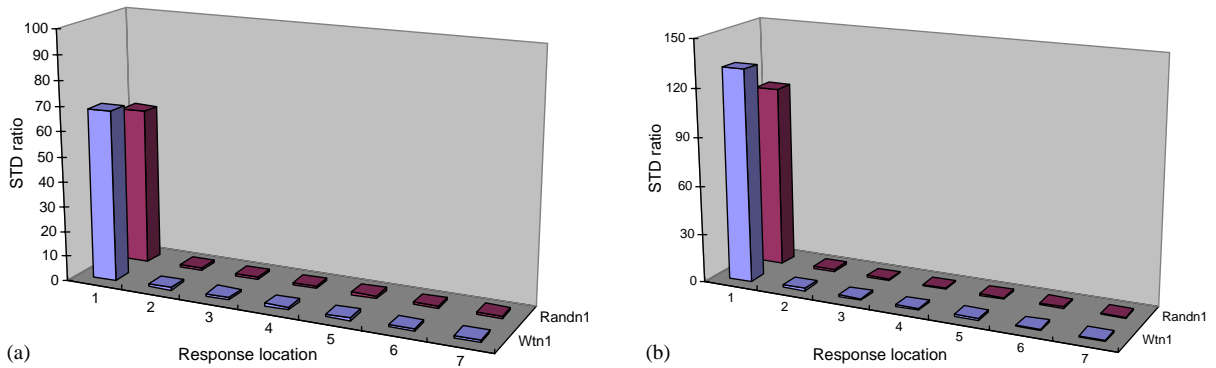


Fig. 6. STD ratio ($\sigma(e_m)/\sigma(e_0)$) for damage case-d (20% reduction of k_1). Using m_8 as ARX model “input”: (a) by base excitation; (b) by force excitation at m_8 .

where $\bar{y}(k) = \{y_1(k), \dots, y_7(k)\}^T$. Accordingly, for the force excitation scheme, the random force is to be applied at point m_8 .

Fig. 6 shows the STD ratios for damage case-d with the above new ARX model under a random base excitation, or a force excitation at m_8 . The location of the damage at k_1 , which is near the base but far away from the new “input” response location (m_8), can now be clearly identified.

Further investigation will be necessary to more clearly understand the physical reasons for the above phenomenon. For practical applications, it is recommended that two runs of the procedure be carried out as illustrated above to ensure a sound diagnosis of damage in An mdof system.

4. Conclusions

A new method for damage diagnosis using time-series analysis of vibration signals is presented in this paper. The method is based on linear dynamic equations and is formulated in a novel form of ARX model with acceleration response signals. The model coefficients relate closely to the dynamic properties of the system, thus enabling the construction of sensitive features for the diagnosis of damage. The model is also disassociated from the input excitation, and this further enhances the potential robustness of the method in real-life applications.

The standard deviation (STD) of the residual error, which is the difference between the measured signals from any actual state of the system and the predicated signals from the ARX model established from a reference (undamaged) state, is found to be a damage-sensitive feature. Numerical simulation studies demonstrate that using the standard deviation of the residual errors as a feature, the occurrence of damage can be detected; and moreover, in an mdof system the location of damage can also be identified as larger STD of the residual errors tend to occur near the actual damage locations.

It is observed that the behavior of the proposed ARX model can be complicated when the location of the response point selected as the ARX model input is near the location of the damage. For this reason, it is recommended that in the diagnosis of an mdof system two separate runs of

the procedure be carried out using two different “input” response locations. A correct detection of the damage location can be achieved by inspecting the two sets of the results.

It has to be pointed out that the standard deviation of the residual error of the ARX model, although sensitive to the occurrence of damage, does not give a precise indication of the degree of damage. For comparable scenarios, the trend is consistent; but to allow for quantification of the degree of damage, further research will be required to extend the capacity of the model, probably with a more suitable damage feature. Besides, the behavior of the model in case of a noisy measurement environment also has to be studied in order to implement the model for practical use.

References

- [1] A.D. Raath, A new time-domain parametric dynamic system identification approach to multiaxial service load simulation testing in components, *International Journal of Fatigue* 19 (5) (1997) 409–414.
- [2] T. Saito, H. Yokota, Evaluation of dynamic characteristics of high-rise buildings using system identification techniques, *Journal of Wind Engineering and Industrial Aerodynamics* 59 (1996) 299–307.
- [3] J. Lardies, N. Larbi, A new method for model order selection and model parameter estimation in time-domain, *Journal of Sound and Vibration* 245 (2) (2001) 187–203.
- [4] S.A. Neild, P.D. McFadden, M.S. Williams, A review of time-frequency methods for structural vibration analysis, *Engineering Structures* 25 (6) (2003) 713–728.
- [5] C.S. Huang, Structural identification from ambient vibration measurement using the multivariate AR model, *Journal of Sound and Vibration* 241 (3) (2001) 337–359.
- [6] X. He, G. De Roeck, System identification of mechanical structures by a high-order multivariate autoregressive model, *Computers and Structures* 64 (1–4) (1997) 341–351.
- [7] C.-F. Hung, W.-J. Ko, Y.-T. Peng, Identification of modal parameters from measured input and output data using a vector backward auto-regressive with exogeneous model, *Journal of Sound and Vibration* 276 (3–5) (2004) 1043–1063.
- [8] C.-G. Lee, C.-B. Yun, Parameter identification of linear structural dynamic systems, *Computers and Structures* 40 (6) (1991) 1475–1487.
- [9] S.F. Masri, M. Nakamura, A.G. Chassiakos, T.K. Caughey, Neural network approach to detection of changes in structural parameters, *Journal of Engineering Mechanics* 122 (4) (1996) 350–360.
- [10] H. Sohn, C.R. Farrar, Damage diagnosis using time series analysis of vibration signals, *Smart Materials and Structures* 10 (2001) 1–6.
- [11] J.-N. Juang, *Applied System Identification*, Prentice-Hall, Englewood Cliffs, NJ, 1994.
- [12] C.L. Phillips, H.T. Nagle, *Digital Control System Analysis and Design*, Prentice-Hall, Englewood Cliffs, NJ, 1984.
- [13] L. Ljung, *System Identification: Theory for the User*, Prentice-Hall, Englewood Cliffs, NJ, 1987.
- [14] G.H. Golub, C.F. Van Loan, *Matrix Computation*, Johns Hopkins University Press, Baltimore, MD, 1983.